Geometric Modeling of End Mills

Puneet Tandon[1], Phalguni Gupta[2] and Sanjay G. Dhande[3]

[1]National Institute of Technology Kurukshetra, puneet.tandon@nitkkr.ac.in
[2]Indian Institute of Technology Kanpur, pg@iitk.ac.in
[3] Indian Institute of Technology Kanpur, sgd@iitk.ac.in

ABSTRACT

Representations of geometries of cutting tools are usually two-dimensional in nature. This paper outlines a detailed geometric model for a variety of end mills and establishes a new three-dimensional definition for its geometry in terms of biparametric surface patches. The work presents the unified models of end mills with different end geometries. The surfaces meant for cutting operations, known as flutes, are modeled as helicoidal surfaces. For the purpose, sectional geometry of tip-to-tip profile is developed and then swept appropriately. The geometric model of shanks and variety of end geometries are developed separately. The transitional surfaces are modeled as bicubic Bézier surfaces or biparametric sweep surfaces. The relations to map proposed three-dimensional angles to conventional angles (forward mapping) and their reverse relations (inverse mapping) are also developed here. The new paradigm offers immense technological advantages in terms of numerous downstream applications.

Keywords: Geometric Modeling, Surface Modeling, End Mills, Tool Geometry, Mapping.

1. INTRODUCTION

Geometry of cutting tool surfaces is one of the crucial parameters affecting the quality of the manufacturing process. Traditionally, the geometry of cutting tools has been defined using the principles of projective geometry. The parameters of geometry defining the various cutting tool angles are described by means of taking appropriate projections of the cutting tool surfaces. Several standards such as ISO, ASA, DIN, BS have been established for specifying the geometry of cutting tools. The developments in the field of Computer Aided Geometric Design (CAGD) now provide a designer to specify the cutting tool surfaces as biparametric surface patches. Such an approach provides the comprehensive three-dimensional (3D) definitions of the cutting tools. The surface model of a cutting tool can be converted into a solid model and used for the Finite Element based engineering analysis, stress analysis and simulation of the cutting tools. The primary goal of this work is to outline geometric models of surface patches for end mills. Further, the relationship between such a geometric model and conventional specification scheme have been established and the surface based definitions of cutting tools have been verified by designing and rendering them in terms of 3D geometric parameters. It is also shown that the 3D geometric definition of the cutting tool provides quickly the data required for numerous downstream applications.

Methodologies in geometric modeling have been found to be successful in specifying the geometry of complex surfaces. The biparametric surface definitions provide extensive freedom for designing complex surfaces [5], [8]. In many practical situations a component is broken up into different surface patches and each patch is defined over a limited region. It is necessary to ensure the continuity conditions of position, tangency, curvature, etc. between adjacent surface patches [1]. Based on the availability of these surface definitions as well as the geometric nature of the cutting tools it has been found that the geometric modeling of the cutting tool as a collection of biparametric surfaces would help the design, analysis as well as manufacturing processes of cutting tools.

A wide range of cutters used in practice is fluted in geometry. Among fluted cutters considerable work has been done in the area of geometric modeling of the drill and helical milling cutters for their design, analysis and grinding. However, modeling of end mills has not received much attention. End mills are cylindrical cutters with teeth on the circumferential surface and one of the ends for chip removal [2], [3], [12]. Whatever work is done on modeling end mills it is not in the direction of development of unified representation schemes that can provide direct 3D models for technological applications. Tandon et al. have proposed the unified modeling schemes for single-point cutting tools [11] and side-milling cutters [10].

In the present work, mathematical models of the complex geometry of the end mills are formulated as a combination of surface patches using the concept of computational geometry. The model is generated keeping in mind that it is to be used for direct analysis, prototyping, manufacturing and grinding of cutters. The orientation of the surface patches is defined in a right hand coordinate frame of reference by 3D angles, termed as rotational angles. The cutters are modeled by sweeping the sectional profile of the cutter along the perpendicular direction. Several application programs to calculate the conventional two-dimensional (2D) tool angles and the rotational angles from one to other are developed. Besides, output in the form of rendered image of a cutter is shown for verification of the methodology.
Section 2 of the manuscript describes the surface modeling of a tooth of flat end mill while surface models of body and blending surfaces are presented in Section 4. The schema for mapping the angles between the existing 2D standards and the proposed 3D nomenclature for an end mill is discussed in Section 4. Section 5 instantiates modeling of an end mill for validation of the methodology, while Section 6 describes one of the down-stream applications of the 3D model as a case study. Finally, concluding remarks are presented in the last section.

2. SURFACE MODELING OF FLAT END MILL TOOTH

End milling cutters are multi-point cutters with cutting edges both on the end face and the circumferential surface of the cutter [2], [3]. The teeth can be straight or helical. End mills combine the abilities of end cutting, peripheral cutting and face milling into one tool. The end mills have straight or tapered shank for mounting and driving. Used vertically, the end mill can plunge cut a counter bore or face mill a slot. When used horizontally in a peripheral milling operation, the end mill's flute length limits the width of the cut. End mills can be used for various operations like facing, slotting, profiling, die sinking, engraving etc. End mills can be classified according to

1. Configuration of end profile - Flat, Chamfer, Radius, Ball, Taper, Bull Nose end mills and their combinations
2. Shank type - Straight shank and Brown and Sharpe or Morse Taper shank
3. Mounting type - Cylindrical, cylindrical threaded, cylindrical power chuck, Weldon threaded

In the present work, a generic flat end mill is modeled. Other profiles of the end mills can be developed from this generic model. For example, for radius end mill, the value of radius is the additional parameter required to model it. The geometry of a flat end mill projected on two-dimensional planes is shown in Fig. 1. The geometry of an end mill may consist of two classes, namely

- Geometry of fluted shank
- End surface geometry

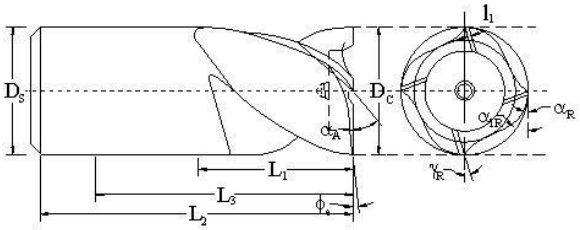

Fig. 1. Two-Dimensional Projected Geometry of End Mill

The geometry of fluted shank consist of circumferential surface patches formed by sweeping the profile of a section, perpendicular to the axis of the cutter. The end geometry depends on the configuration of the end profile. A single tooth of the end mill is modeled with the help of nine surface patches, labeled Σ_1 to Σ_9. Tab. 1 lists the surface patches of a tooth of the flat end mill. The schematic figure of the tooth of the right hand, right helix flat end mill is shown with the help of Fig. 2 [12].

Symbol	Surface Patch Name	Symbol	Surface Patch Name
Σ_1	Face	Σ_6	Fillet
Σ_2	Peripheral Land	Σ_7	Face Land
Σ_3	Heel or Secondary Land	Σ_8	Minor Flank
Σ_4	Blending Surface	Σ_9	Rake Face Extension
Σ_5	Back of Tooth		

Tab. 1 Surface Patches of End Mill

2.1 Geometry of Fluted Shank

Surfaces Σ_1 to Σ_6 are the surface patches on the fluted shank. These surfaces are formed as helicoidal surfaces. Helicoidal surfaces are formed when a composite curve in XY plane is swept with a sweeping rule, composed of combined rotational and parallel sweep. The composite sectional curve ($V_1 \ldots V_7$) at the cutting end is composed of six segments and is shown in Fig. 3. Segments V_1V_2, V_2V_3 and V_6V_7 of the composite curve are straight lines, while segments V_3V_4, V_4V_5 and V_5V_6 are circular arcs of radii r_3, r_2 and R respectively. Out of these six, three segments V_1V_2, V_2V_3 and V_6V_7 correspond to the three land widths, namely peripheral land, heel and face, and are shown as straight lines on a two-dimensional projective plane. The other three segments are circular arcs in geometry and correspond to fillet, back of tooth and blending surface.

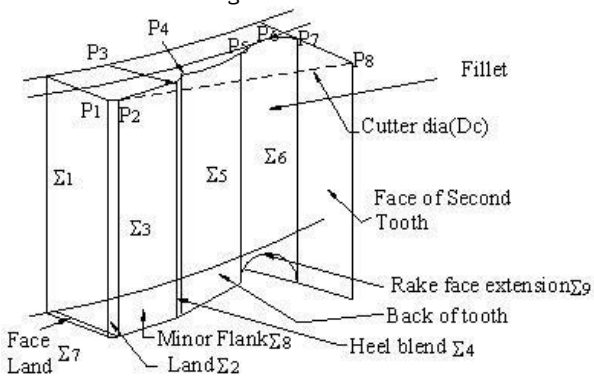

Fig. 2. Modeling of an End Mill Tooth

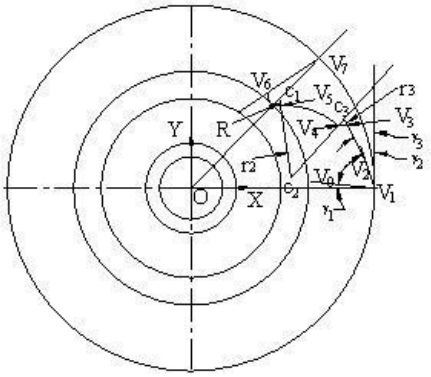

Fig. 3. Composite Sectional Curve

To model the cross-sectional profile in two-dimensional plane, the input parameters are (i) widths of lands i.e. peripheral land, heel or secondary land and face given by l_1, l_2 and l_3 respectively, (ii) 3D angles obtained to form face (γ_1), land (γ_2) and heel (γ_3) about Z axis, (iii) radii of fillet (R), back of tooth (r_2) and blending surface (r_3), (iv) diameter of cutting end of the end mill (D_c) and (v) number of flutes (N). Besides, the length and angle of chord represented by l_4 and γ_4 respectively, joining the end vertices V_3 and V_4 of blending surface are also known.

In a Cartesian coordinate frame of reference C_1, with center of the end mill's cross section coinciding with origin, the position vectors of end vertices of different sections of the composite profile curve and center points of the three circular arcs (c_1, c_2, c_3) are satisfied by the following relations

$$\mathbf{v}_1 = \left[\frac{D_c}{2} \quad 0 \quad 0 \quad 1\right]$$

$$\mathbf{v}_2 = \left[\left(\frac{D_c}{2} - l_1 \sin\gamma_2\right) \quad l_1 \cos\gamma_2 \quad 0 \quad 1\right]$$

$$\mathbf{v}_3 = \left[\left\{\frac{D_c}{2} - (l_1 \sin\gamma_2 + l_2 \sin\gamma_3)\right\} \quad (l_1 \cos\gamma_2 + l_2 \cos\gamma_3) \quad 0 \quad 1\right]$$

$$\mathbf{v}_4 = \left[\left\{\frac{D_c}{2} - (l_1 \sin\gamma_2 + l_2 \sin\gamma_3 + l_4 \sin\gamma_4)\right\} \quad (l_1 \cos\gamma_2 + l_2 \cos\gamma_3 + l_4 \cos\gamma_4) \quad 0 \quad 1\right]$$

$$\mathbf{v}_5 = \left[\left\{\frac{D_c}{2}\cos\psi - l_3 \cos(\psi+\gamma_1) + R(\sin(\psi+\gamma_1) + \cos\theta_1)\right\} \quad \left\{\frac{D_c}{2}\sin\psi - l_3 \sin(\psi+\gamma_1) - R(\cos(\psi+\gamma_1) + \sin\theta_1)\right\} \quad 0 \quad 1\right]$$

$$\mathbf{v}_6 = \left[\left\{\frac{D_c}{2}\cos\psi - l_3 \cos(\psi+\gamma_1)\right\} \quad \left\{\frac{D_c}{2}\sin\psi - l_3 \sin(\psi+\gamma_1)\right\} \quad 0 \quad 1\right]$$

$$\mathbf{v}_7 = \left[\frac{D_c}{2}\cos\psi \quad \frac{D_c}{2}\sin\psi \quad 0 \quad 1\right]$$

$$\mathbf{c}_1 = \left[\left\{\frac{D_c}{2}\cos\psi - l_3 \cos(\psi+\gamma_1) + R\sin(\psi+\gamma_1)\right\} \quad \left\{\frac{D_c}{2}\sin\psi - l_3 \sin(\psi+\gamma_1) - R\cos(\psi+\gamma_1)\right\} \quad 0 \quad 1\right]$$

$$\mathbf{c}_2 = \left[\left\{ \frac{D_c}{2} - (l_1 \sin\gamma_2 + l_2 \sin\gamma_3 + l_4 \sin\gamma_4) - r_2 \cos\theta \right\} \quad \left\{ (l_1 \cos\gamma_2 + l_2 \cos\gamma_3 + l_4 \cos\gamma_4 - r_2 \sin\theta) \right\} \quad 0 \quad 1 \right]$$

$$\mathbf{c}_3 = \left[\left\{ \frac{D_c}{2} - (l_1 \sin\gamma_2 + l_2 \sin\gamma_3) - r_3 \sin(\gamma_4 - \phi) \right\} \quad \left\{ (l_1 \cos\gamma_2 + l_2 \cos\gamma_3 + r_3 \cos(\gamma_4 - \phi) \right\} \quad 0 \quad 1 \right]$$

where $\psi = 2\pi/N$, $\phi = \cos^{-1}\left(\frac{l_4}{2r_3}\right)$, $\theta = \tan^{-1}\left(\frac{c_{3y} - v_{4y}}{c_{3x} - v_{4x}}\right)$ and $\theta_1 = \tan^{-1}\left(\frac{c_{1y} - c_{2y}}{c_{1x} - c_{2x}}\right)$, with the condition that

if $\theta_1 < 0$, then $\theta_1 = \pi + \theta_1$
else $\theta_1 = \theta_1$

2.2 Modeling of Fluted Surfaces of End Mill

As discussed earlier, the cross-section profile of an end mill consists of three parametric linear edges and three parametric circular edges, namely, $\mathbf{p}_1(s)$ to $\mathbf{p}_6(s)$. Edges $\mathbf{p}_1(s)$, $\mathbf{p}_2(s)$ and $\mathbf{p}_6(s)$ are straight edges and $\mathbf{p}_3(s)$, $\mathbf{p}_4(s)$ and $\mathbf{p}_5(s)$ are circular in two-dimensional space. The generic definition of the sectional profile in XY plane in terms of parameter *s* may be represented by

$$\mathbf{p}_i(s) = [\mathbf{f_{i1}}(s) \quad \mathbf{f_{i2}}(s) \quad 0 \quad 1]$$

The fluted surface is obtained by combined rotational and parallel sweeping. The helix angle remains constant on the cylindrical shank. The helicoidal surface for fluted shank is parametrically described by

$$\mathbf{p}(s,\phi) = \mathbf{p}(s).[\mathbf{T_S}], \text{ where}$$

$$T_S = \begin{bmatrix} \cos\phi & \sin\phi & 0 & 0 \\ -\sin\phi & \cos\phi & 0 & 0 \\ 0 & 0 & 1 & 0 \\ 0 & 0 & \frac{P\phi}{2\pi} & 1 \end{bmatrix} \text{ for } 0 \le \phi \le \frac{2\pi L}{P}$$

In the above equation, L is the length of fluted shank. The length may be equal to L_1 for flat end mills and (L_1-D_c/2) for ball end mills.

Sweeping Rules

The fluted section of an end mill can have right helix or left helix. If the flute's spiral have a clockwise contour when looked along the cutter axis from either end, then it is a right helix else helix is left [2], [3]. For a right helix cutter, the cross-section curve rotates by an angle $+\phi$ about the axis in right hand sense. Three different sweeping rules can be formulated for the fluted shank and the end profile of the cutter. These rules are for

(i) Cylindrical Helical Path
(ii) Conical Helical Path
(iii) Hemispherical Helical Path

Cylindrical Helical Path - The path when the composite profile curve is swept helically along a cylinder is known as cylindrical helical path. For a helical cutter let ϕ be the parameter denoting the angular movement, P the pitch of the helix, D_c the cylindrical cutter diameter and L_1 the length of the cutter, then the mathematical definition of the helix is $x = (D_c/2).\cos\phi$, $y = (D_c/2).\sin\phi$ and $z = (P\phi)/(2\pi)$, where $0 \le \phi \le (2\pi L_1/P)$.

Conical Helical Path - The helical path along a frustum of cone of cutting end diameter D_c and shank side diameter D_s is defined by $x = (D/2).\cos\phi$, $y = (D/2).\sin\phi$ and $z = (P\phi)/(2\pi)$, where $D = D_c + (D_s\text{-}D_c)z/L_1$ and $0 \le \phi \le (2\pi L_1/P)$. This is valid for both types of frustum of cones i.e. when $D_c < D_s$ and when $D_c > D_s$.

Hemispherical Helical Path - The helical path along the hemispherical object of diameter D_c is given as $x=(D/2).\cos\psi\cos\phi$, $y = (D/2).\cos\psi\sin\phi$, and $z = (D_c/2).(1\text{-}\sin\psi)$, where $0 \le \phi \le \pi D_c/P$ and $0 \le \psi \le \pi/2$. Here, ϕ is the angle about Z axis and ψ is the angle with XY plane and the relation between them is $\psi = \sin^{-1}\left[1 - \frac{P\phi}{D_c\pi}\right]$.

2.3 End Surface Geometry

The end geometry of a fluted end mill depends upon the end mill profile configuration. For example, in the case of the flat end mill, the end consists of three planes and one blending surface. The planes are (i) Face Land Σ_7, (ii) Minor Flank, Σ_8 and (iii) rake face extension, Σ_9, whereas the blending surface blends surface patch Σ_8 of the first tooth with surface Σ_9 of the second tooth of the end mill (labeled as ${}^2\Sigma_9$).

Face land (Σ_7) is formed when an XY plane given by [u_7 v_7 0 1] is transformed through rotation by an angle α_7 about X axis [$R_{x,\alpha 7}$], followed by rotation by an angle γ_1 about Z axis [$R_{z,\gamma 1}$]. The surface Σ_7 is defined as

$$\mathbf{p}_7(u_7, v_7) = \begin{bmatrix} (u_7 \cos\gamma_1 - v_7 \cos\alpha_7 \sin\gamma_1) & (u_7 \sin\gamma_1 + v_7 \cos\alpha_7 \cos\gamma_1) & v_7 \sin\alpha_7 & 1 \end{bmatrix} \quad (1)$$

Minor Flank (Σ_8) is formed when an XY plane is rotated by an angle α_8 about X axis [$R_{x,\alpha 8}$], followed by an angle γ_1 about Z axis [$R_{z,\gamma 1}$], and then translated by a distance d_{82} ($=l_1\cos\gamma_2$) along Y axis and d_{83} ($=l_1\cos\gamma_2\sin\alpha_7$) along Z direction [$\mathbf{T}_{yz}$]. The surface Σ_8 is given as

$$\mathbf{p}_8(u_8, v_8) = \begin{bmatrix} (u_8 \cos\gamma_1 - v_8 \cos\alpha_8 \sin\gamma_1) & (u_8 \sin\gamma_1 + v_8 \cos\alpha_8 \cos\gamma_1 + d_{82}) & (v_8 \sin\alpha_8 + d_{83}) & 1 \end{bmatrix} \quad (2)$$

An ZX plane ([u_9 0 w_9 1]), forms rake face extension Σ_9 when rotated by an angle α_9 about X axis [$R_{x,\alpha 9}$] and by an angle γ_1 about Z axis [$R_{z,\gamma 1}$]. Here, helix angle $\lambda = \tan^{-1}(P/\pi D_c)$, $\alpha_9 = 90°-\lambda^*$ and $\lambda^* = \lambda+(15°-25°)$ but $\leq 90°$. The surface Σ_9 satisfies the relation

$$\mathbf{p}_9(u_9, w_9) = \begin{bmatrix} (u_9 \cos\gamma_1 - w_9 \sin\alpha_9 \sin\gamma_1) & (u_9 \sin\gamma_1 + w_9 \sin\alpha_9 \cos\gamma_1) & w_9 \cos\alpha_9 & 1 \end{bmatrix} \quad (3)$$

2.4 Ball End Mill Cutter

Similar to flat end mills, the geometry of ball end mills is also made of fluted shank and end portion geometry. The fluted shank geometry is similar for all types of end mills but the end geometry differs. In the case of ball end mill, the end geometry is also fluted in nature. For end portion of the ball end mill, each flute lies on the surface of the hemisphere, and is ground with a constant helix lead [6], [7]. The radius of the ball in XY planes reduces along the cutter axis towards cutting end, as the tip of the hemisphere lies in contact with work surface. Due to this, the local helix angle varies along the cutting flute.

The diameter of the cross section of the hemispherical ball is a function of z, which varies from 0 at the tip of the ball part to D_c at the meeting of ball and shank boundary. The radius of cross-section at any instance z, is $r(z) = (D_c z - z^2)^{1/2}$, where $z = P\phi/(2\pi)$ and $0 \leq \phi \leq \pi D_c/P$. The ratio by which the cross-section reduces while moving towards the tip of the ball end mill is $(2r(z)/D_c)$.

2.5 Conical End Milling Cutter

In conical end mills, similar to ball end mills, the end portion is fluted. To obtain the fluted end geometry, the radius of cross-section $r(z)$ for conical end portion satisfies the relation $r(z) = D_c z/(2h)$, where h is the height of the conical end.

3. MODELING OF BODY AND BLENDING SURFACES

The cutter body of end mill consists of a shank, which may be modeled as a combination of two surface patches. These surface patches are (i) cylindrical surface of revolution Σ_{50} and (ii) planar end surface Σ_{51}. The cylindrical surface of shank may be parametrically defined by

$$\mathbf{p}_{50}(w, \phi) = \begin{bmatrix} \frac{D'}{2}\cos\phi & \frac{D'}{2}\sin\phi & \{L_1 + w(L_2 - L_1)\} & 1 \end{bmatrix} \quad (4)$$

for $0 \leq \phi \leq 2\pi$, $0 \leq w \leq 1$. The term L_2 stands for overall length of end mill and diameter D' may be given by

$$D' = \begin{cases} \frac{D_s}{2}, & \text{for straight shank} \\ \frac{D_c}{2} + w\frac{D_s - D_c}{2}, & \text{for tapered shank} \end{cases}$$

The planar end surface forming the end opposite to cutting end is parametrically modeled as

$$\mathbf{p}_{51}(u, v) = \begin{bmatrix} u & v & L_2 & 1 \end{bmatrix} \text{ for } -\infty \leq u, v \leq \infty \quad (5)$$

The only blending surface on the body of the cutter is a unit width, 45° chamfer between body surface patches Σ_{50} and Σ_{51}. The chamfer $\sigma_{50,51}$ is modeled as a surface of revolution. The coordinates of the two end points of the edge that is revolved about Z axis to form the chamfer are $((D_s/2-0.707), 0, L_2)$ and $(D_s/2, 0, (L_2-0.707))$. The chamfer is given by

$$\sigma_{50,51}(u, \theta) = \begin{bmatrix} \left\{\frac{D_s}{2} - 0.707(1-u)\cos\theta\right\} & \left\{\frac{D_s}{2} - 0.707(1-u)\sin\theta\right\} & (L_2 - 0.707u)\} & 1 \end{bmatrix} \quad (6)$$

for $0 \leq u \leq 1$ and $0 \leq \theta \leq 2\pi$.

4. MAPPING RELATIONS

This section establishes a set of relations that map the three-dimensional (3D) rotational angles proposed in this paper to define the geometry of end mills into traditional two-dimensional angles defined by traditional nomenclatures and vice versa. The former is called forward mapping while the latter is known as inverse mapping. The conventional angles are formed by projecting the surface patches of the end mill on planes and the traditional geometry of end mill can be referred from [2], [3]. Mapping guide table (Tab. 2) shows the methodology of expressing the formation of conventional angles. The forward mapping relations are:

Conventional Angles	Formed by	About the Plane	Plane of Projection
γ_R	Σ_1	ZX	XY
α_R	Σ_2	YZ	XY
α_{1R}	Σ_3	YZ	XY
ϕ_e	Σ_7	XY	ZX
α_A	Σ_7	XY	YZ

Tab. 2. Mapping Guide Table for End Mill

Radial Rake Angle (γ_R): Rake face Σ_1 forms radial rake angle (γ_R) with ZX plane. This angle is expressed when projected to XY plane. The plane Σ_1 is formed by the edge ($\mathbf{e}_{01}$) joining vertex V_0 to V_1, when swept by transformation matrix [$\mathbf{T}_s$]. In terms of homogenous coordinates the edge $\mathbf{e}_{01}$ is expressed as [{D_c/2-$l_3$cosγ_1(1-s)} -$l_3$sinγ_1(1-s) 0 1]. The mathematical equation of Σ_1 is given by

$$\mathbf{p}_1(s,\phi) = \mathbf{e}_{01}.[\mathbf{T}_s]$$
$$= \left[\left\{ (\frac{D_c}{2} - (1-s)l_3 \cos\gamma_1)\cos\phi + (1-s)l_3 \sin\gamma_1 \sin\phi \right\} \quad \left\{ (\frac{D_c}{2} - (1-s)l_3 \cos\gamma_1)\sin\phi - (1-s)l_3 \sin\gamma_1 \cos\phi \right\} \quad \frac{P\phi}{2\pi} \quad 1 \right]$$

The tangent vectors $\frac{\partial \mathbf{p}_1}{\partial s}, \frac{\partial \mathbf{p}_1}{\partial \phi}$ to rake face Σ_1 are found by differentiating above equation with respect to parameters *s* and ϕ and the vector normal to the surface Σ_1 is

$$\mathbf{n}_1 = \frac{Pl_3}{2\pi}\sin(\gamma_1+\phi)\hat{i} - \frac{Pl_3}{2\pi}\cos(\gamma_1+\phi)\hat{j} + \left[\frac{D_c}{2} l_3 \cos\gamma_1 - (1-s)l_3^2 \right]\hat{k}$$

To find radial rake angle γ_R, $\mathbf{n}_1$ is projected on XY plane ($\mathbf{n}_{1P}$) and unit projected normal vector ($\hat{n}_{1P}$) is evaluated as $\hat{n}_{1P} = \mathbf{n}_{1p} \big/ \left|\mathbf{n}_{1p}\right| = \sin(\gamma_1+\phi)\hat{i} - \cos(\gamma_1+\phi)\hat{j}$.

Radial rake angle is found by taking scalar product of $\hat{n}_{1P}$ with unit vector $\hat{j}$, as this is similar to the angle between normal to face Σ_1, projected on XY plane and Y axis i.e. cos γ_R = -cos (γ_1+ϕ). At z=0 plane, ϕ=0, and hence $\gamma_R = -\gamma_1$.

Radial Relief Angle (α_R): Radial relief Angle is formed by land Σ_2 about YZ plane when projected on XY plane. The land Σ_2 can be geometrically expressed by

$$\mathbf{p}_2(s,\phi) = \left[\left\{ (\frac{D_c}{2} - sl_1 \sin\gamma_2)\cos\phi - sl_1 \cos\gamma_2 \sin\phi \right\} \quad \left\{ (\frac{D_c}{2} - sl_1 \sin\gamma_2)\sin\phi + sl_1 \cos\gamma_2 \cos\phi \right\} \quad \frac{P\phi}{2\pi} \quad 1 \right]$$

The tangents to Σ_2 at any arbitrary point are $\mathbf{p}_{2s}(s,\phi)$ and $\mathbf{p}_{2\phi}(s,\phi)$. The unit normal to surface Σ_2 projected on XY plane is $\hat{n}_{2P} = \cos(\gamma_2+\phi)\hat{i} + \sin(\gamma_2+\phi)\hat{j}$. Angle of surface Σ_2 with YZ plane (Radial Relief Angle) is similar to angle formed by $\hat{n}_{2P}$ with unit vector î. This, on solution, gives cosα_R = cos (γ_2+ϕ). At z=0 plane, ϕ = 0, and hence $\alpha_R = \gamma_2$.

Radial Clearance Angle (α_{1R}): This angle is formed by the flank (Σ_3) of a tooth of end mill with YZ plane when projected on the XY plane. Flank Σ_3 is defined by the relation $\mathbf{p}_3(s,\phi)=\mathbf{p}_2(s).[\mathbf{T}_s]$. The normal to Σ_3 at any arbitrary point is

$$\mathbf{n}_3 = \frac{Pl_2}{2\pi}\cos(\gamma_3+\phi)\hat{i} + \frac{Pl_2}{2\pi}\sin(\gamma_3+\phi)\hat{j} + \left\{ -\frac{D_c}{2} l_2 \sin\gamma_3 + l_1 l_2 \cos(\gamma_3-\gamma_2) + sl_2^2 \right\}\hat{k}$$

This normal on projection to XY plane leads $\hat{n}_{3P} = \cos(\gamma_3+\phi)\hat{i} + \sin(\gamma_3+\phi)\hat{j}$. Radial clearance angle is similar to the angle formed by $\hat{n}_{3P}$ with unit vector normal to YZ plane. This gives cosα_{1R} = cos (γ_3+ϕ) or $\alpha_{1R} = \gamma_3$ at ϕ = 0.

Axial Relief Angle (α_A): It is formed by the surface patch Σ_7, given by

$$\mathbf{p}_7(u_7, v_7) = \begin{bmatrix} (u_7 \cos\gamma_1 - v_7 \cos\alpha_7 \sin\gamma_1) & (u_7 \sin\gamma_1 + v_7 \cos\alpha_7 \cos\gamma_1) & v_7 \sin\alpha_7 & 1 \end{bmatrix}$$

The normal to this surface is $\mathbf{n}_7 = \sin\gamma_1 \sin\alpha_7 \hat{i} - \cos\gamma_1 \sin\alpha_7 \hat{j} + \cos\alpha_7 \hat{k}$. The projection of this normal vector on YZ plane is $\hat{n}_{7P} = -\cos\gamma_1 \sin\alpha_7 \hat{j} + \cos\alpha_7 \hat{k}$. Scalar product of unit vector $\hat{n}_{7P}$ with unit vector $\hat{k}$ gives the angle α_A as:

$$\alpha_A = \cos^{-1}\left[\frac{\cos\alpha_7}{\sqrt{\cos^2\gamma_1 \sin^2\alpha_7 + \cos^2\alpha_7}}\right]$$

End Cutting Edge Angle (ϕ_e): This angle is formed by the surface patch Σ_7 with XY plane and is measured when projected on ZX plane. This angle is equivalent to the angle between the unit vectors normal to Σ_7 and to XY plane, when projected on ZX plane. The angle is computed by taking the scalar product of unit normal vector projected on ZX plane and unit vector $\hat{k}$ and given by the relation

$$\phi_e = \cos^{-1}\left[\frac{\cos\alpha_7}{\sqrt{\sin^2\gamma_1 \sin^2\alpha_7 + \cos^2\alpha_7}}\right]$$

Inverse Mapping:

This constitutes a set of relations, which maps the given conventional 2D angles in terms of proposed 3D angles. Once the inverse mapping relations and conventional angles are available, it is very convenient to find the rotational angles. The forward mapping relations for end mills are summarized in Tab. 3.

Conventional Angles		Rotational Angles
Radial Rake Angle, $\pm\gamma_R$	=	$\mp\gamma_1$
Radial Relief Angle, α_R	=	γ_2
Radial Clearance Angle, α_{1R}	=	γ_3
Axial Relief Angle, α_A	=	$\cos^{-1}\left[\frac{\cos\alpha_7}{\sqrt{\cos^2\gamma_1 \sin^2\alpha_7 + \cos^2\alpha_7}}\right]$
End Cutting Edge Angle, ϕ_e	=	$\cos^{-1}\left[\frac{\cos\alpha_7}{\sqrt{\sin^2\gamma_1 \sin^2\alpha_7 + \cos^2\alpha_7}}\right]$

Tab. 3. Forward Mapping Relations for End Mill

Solution of these forward mapping relations establishes inverse mapping that helps to evaluate the 3D rotational angles if tool angles specified by conventional nomenclatures are known. Tab. 4 presents the inverse mapping for end mills.

Rotational Angles		Conventional Angles
γ_1	=	$-\gamma_R$
γ_2	=	α_R
γ_3	=	α_{1R}
α_7	=	$\cos^{-1}\left[\frac{\cos\alpha_A . \cos\phi_e}{\sqrt{\cos^2\alpha_A + \cos^2\phi_e - \cos^2\alpha_A \cos^2\phi_e}}\right]$

Tab. 4. Inverse Mapping Relations for End Mill

5. VALIDATION

This section presents an example on geometric modeling of an end mill on the basis of 3D geometric parameters. The 3D parameters used to construct the model of slab mill are referred in *ANSI/ASME B94.19-1985* standards. The geometric parameters of the cutter used for rendering, to validate the approach of modeling of cutters in terms of 3D

parameters is presented in Tab. 5 [9]. The resultant cutter is rendered in OpenGL environment [13] and shown with the help of Fig. 4.

Input Data for End Mill			
Dimensional Parameters	Value (mm)	Rotational Angles	Value (degrees)
Cutter Diameter (D_C)	25.0	γ_1	-5.0
Length of Cutter (L)	131.0	γ_2	5.0
Length of Flutes (L_1)	71.0	γ_3	15.0
Root Diameter (D_R)	6.0	α_7	75.0
Shank side Diameter (D_S)	25.0		
Number of Flutes (N)	4		
Pitch (P)	450.0		

Tab. 5. Geometric Parameters of End Mill

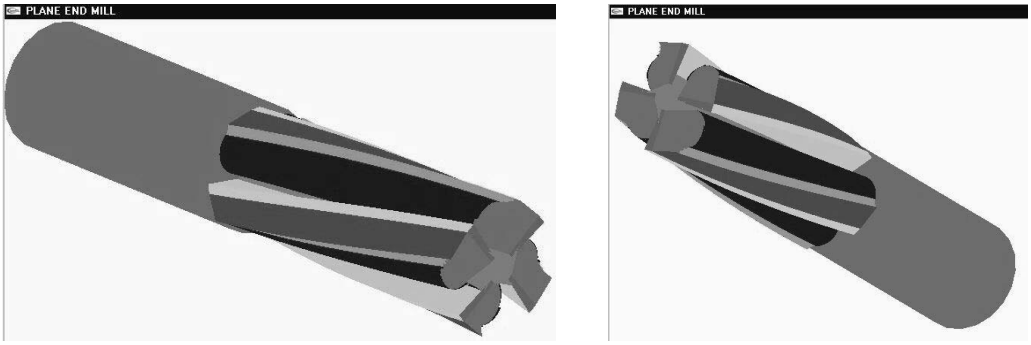

Fig. 4. Rendering of an End Mill

6. CASE STUDY

This paper illustrates the development of comprehensive 3D models of end mills. The inputs to the models are 3D geometric parameters. The models developed can be imported into any surface or solid modeling environment and subjected to a wide range of down-stream applications. This section presents an exercise on finite element based engineering analysis (FEA) on the 3D model of the end mill. This case study highlights the advantages and utilities unfolded, once a comprehensive 3D definition of the cutter is available. The purpose here is not to present any detailed analysis of end mill during machining. The 3D CAD model of the cutter is imported through ASCII file format in one of the commercial CAD/Analysis software and a wide range of analysis (e.g. static, dynamic, impact, fatigue, thermal etc.) for stress, wear, deflection etc. can be performed on it using the tools of the software. The present case study models the static and impact analysis carried out on the two flute of the end mill using I-DEAS [4]. The impact analysis can be useful for high speed machining applications. Fig. 5 shows the resultant stress and displacement distribution at one of the corners of the major cutting edge of the end mill.

7. CONCLUSIONS

The geometric modeling of the cutting tools is an important aspect for the design and manufacturing engineers from the viewpoint of shape realization. The present work has covered the modeling of the end mill by mathematically expressing the geometry of the cutting tools in terms of various biparametric surface patches. By solving these equations, the surface models of the tools have been realized. These surface models have been converted to solid models and their engineering analysis is carried out using a standard FEA package.

Four 3D rotational angles (γ_1, γ_2, γ_3, α_7) are defined to model an end mill. The mathematical definitions of the surfaces have been used to obtain the standard 2D tool angles from these proposed rotational angles. The inverse relationships to obtain the rotational angles from the conventional angles are also obtained. The model has been developed keeping in mind a Right Hand cutter but a Left Hand cutter can also be similarly generated. The entire exercise is in the direction of proposing a new nomenclature for defining the geometries of fluted cutters and attempts to recast the method of defining a cutting tool in terms of 3D geometric models.

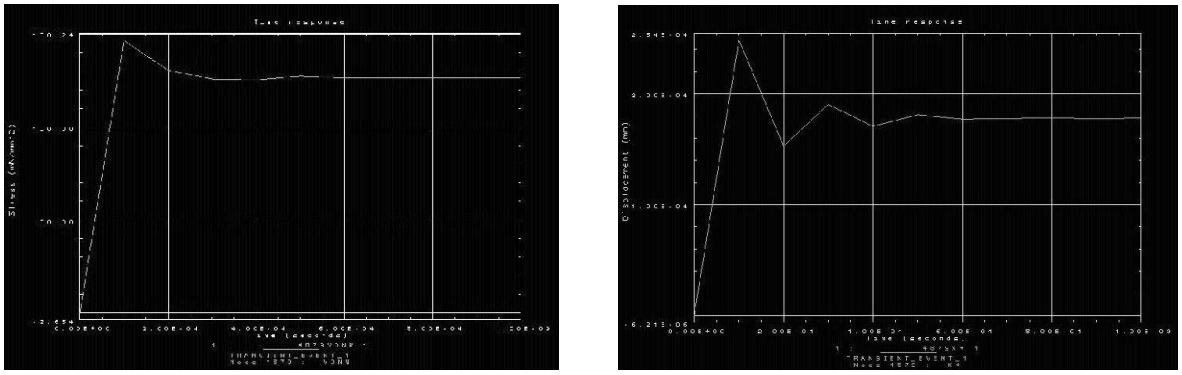

Fig. 5. Stress and Displacement Distribution at the tip of End Mill

Once an accurate biparametric surface model of the cutting tool is evolved it can be used for numerous downstream applications and thus, opens up various probable areas of work. For example, the surface definitions of the tool faces could be used to model mathematically the grinding process and the effect of grinding parameters on the tool geometry can be studied. The above step would enable the entire grinding or sharpening process of the tool to be simulated on the computer and the results verified before any material removal is done.

8. REFERENCES

[1] Choi, B.K., *Surface Modeling for CAD/CAM*, Elsevier, Amsterdam, 1991.

[2] Dallas, D.B., *Tool and Manufacturing Engineers Handbook*, *3rd Ed.,* McGraw-Hill, N.Y., 1976.

[3] Drodza, T.J. and Wick, C., *Tool and Manufacturing Engineers Handbook, Volume I -- Machining*, Society of Manufacturing Engineers, Dearborn, MI, 1983.

[4] I-DEAS Master Series 8, *I-DEAS Students Guide and Training Manual*, SDRC Inc., USA, 1999.

[5] Mortenson, M.E., *Geometric Modeling*, John Wiley & Sons, N.Y., 1985.

[6] Popov, S., Dibner, L. and Kamenkovich, A., *Sharpening of Cutting Tools*, Mir Publishers, Moscow, 1988.

[7] Rodin, P., *Design and Production of Metal Cutting Tools*, Mir Publishers, Moscow, 1968.

[8] Rogers, D.F. and Adams, J.A., *Mathematical Elements of Computer Graphics*, McGraw Hill Publishing Company, 1990, pp.101-141.

[9] SANDVIK, Coromant brazed turning tools catalog.

[10] Tandon, P., Gupta, P. and Dhande, S.G., Geometric Modeling of Side Milling Cutting Tool Surfaces, *International Journal of Engineering Simulation*, Vol. 3, No. 3, 2002, pp. 21-29.

[11] Tandon, P., Gupta, P. and Dhande, S.G., Geometric Modeling of Single Point Cutting Tool Surfaces, *International Journal of Advanced Manufacturing Technology*, Vol. 22, No. 1-2, 2003, pp. 101-111.

[12] Wilson, F.W., 1987, *ASTME: Fundamentals of Tool Design*, Prentice Hall, N.J., 1987.

[13] Woo, M., Neider, J. and Davis, T., *OpenGL Programming Guide,* Addison-Wesley, Reading, MA, 1998.